nature cell biology

Centrosomal MPF triggers the mitotic and morphogenetic switches of fission yeast

Agnes Grallert[1,4], Avinash Patel[1,4], Victor A. Tallada[1,5], Kuan Yoow Chan[1], Steven Bagley[2], Andrea Krapp[3], Viesturs Simanis[3] and Iain M. Hagan[1,6]

Activation of mitosis-promoting factor (MPF) drives mitotic commitment[1]. In human cells active MPF appears first on centrosomes[2]. We show that local activation of MPF on the equivalent organelle of fission yeast, the spindle pole body (SPB), promotes Polo kinase activity at the SPBs long before global MPF activation drives mitotic commitment. Artificially promoting MPF or Polo activity at various locations revealed that this local control of Plo1 activity on G2 phase SPBs dictates the timing of mitotic commitment. Cytokinesis of the rod-shaped fission yeast cell generates a naive, new, cell end. Growth is restricted to the experienced old end until a point in G2 phase called new end take off (NETO) when bipolar growth is triggered[3]. NETO coincided with MPF activation of Plo1 on G2 phase SPBs (ref. 4). Both MPF and Polo activities were required for NETO and both induced NETO when ectopically activated at interphase SPBs. NETO promotion by MPF required polo. Thus, local MPF activation on G2 SPBs directs polo kinase to control at least two distinct and temporally separated, cell-cycle transitions at remote locations.

Mutations in the SPB component Cut12 exhibit a reciprocal relationship with mutations in the MPF-activating phosphatase Cdc25. The loss-of-function mutation *cdc25.22* is suppressed by gain-of-function mutations in *cut12*, such as *cut12.s11* (refs 5,6). Conversely, increased Cdc25 levels suppress the loss-of-function mutant *cut12.1* (ref. 7). The polo kinase Plo1 associates with the SPB towards the end of G2 phase. The timing of this recruitment is advanced in *cut12.s11* cells[4,8]. The antibody MPM2 recognizes SPBs in a Plo1-dependent manner[8] and so offers an ideal tool with which to assess the local activity of Plo1 on the SPB. Unlike bulk *in vitro* kinase assays, MPM2 assessment of Plo1 activity on SPBs is independent of any changes in Plo1 activities at any other locations. MPM2 SPB staining indicates that the Plo1 that associates with SPBs during G2 phase of both wild-type and *cut12.s11* cells is active[8]. Prompted by the fact that the enhancement of Plo1 activity that accompanies mitotic commitment is driven by MPF activation[9], we now address the function of this SPB-associated Plo1 in mitotic control.

MPM2 or Plo1 immunofluorescence staining reveals single (late G2 phase) or paired foci (mitotic) of SPB staining. The ratio of 1:2 foci (G2/Mitotic) in cell populations gives an indication of the point in G2 at which Plo1 is recruited to (Plo1 staining), or activated at (MPM2), SPBs. Staining patterns in an established *plo1.GFP* strain[10] revealed that the fusion of GFP sequences to the carboxy terminus of Plo1 did not alter the timing or activation of Plo1 at SPBs (Fig. 1a). Time-lapse imaging revealed that Plo1 was initially recruited around 30 min before mitosis (Fig. 1a–c). This initial recruitment was advanced by a further 30 min in *cut12.s11* cells (Fig. 1a–c and Supplementary Video S1). Fluorescence recovery after photobleaching (FRAP) revealed a rapid turnover of Plo1.GFP (half-life 21–22 s) at the SPBs of both *cut12*$^{+}$ and *cut12.s11* cells (Fig. 1d and Supplementary Video S2).

To assess the impact of MPF activity on Plo1 SPB recruitment we exploited the *cdc2.as* mutation in the catalytic subunit of MPF that renders it sensitive to inhibition by ATP analogues[11]. *plo1.GFP cdc2*$^{+}$ cells were labelled by transient immersion in fluorescent lectin[12] and mixed with *plo1.GFP cdc2.as* cells for live-cell imaging. Addition of the ATP analogue 1NA-PP1 prompted the immediate loss of Plo1.GFP from G2 SPBs of *cdc2.as* cells whereas it persisted on the G2 SPBs of neighbouring *cdc2*$^{+}$ cells (Fig. 1e,f and Supplementary Videos S3 and S4). Restoration of MPF activity by removal of the analogue promoted a rapid return (Fig. 1f and Supplementary Video S4), indicating that MPF activity is continuously required for Plo1 association with the late G2 SPB.

We extended the analogue-sensitive approach to assess the contribution of Plo1 activity to mitotic control in unperturbed

[1]CRUK Cell Division Group, Paterson Institute for Cancer Research, Wilmslow Road, Manchester, M20 4BX, UK. [2]Advanced Imaging and Flow Cytometry, Paterson Institute for Cancer Research, Wilmslow Road, Manchester, M20 4BX, UK. [3]EPFL SV ISREC UPSIM, SV2.1830, Station 19, CH-1015 Lausanne, Switzerland. [4]These authors contributed equally to this work. [5]Present address: Centro Andaluz de Biología del Desarrollo, Universidad Pablo de Olavide/Consejo Superior de Investigaciones Cientificas, 41013 Sevilla, Spain.
[6]Correspondence should be addressed to I.M.H. (e-mail: ihagan@picr.man.ac.uk)

Received 3 July 2012; accepted 29 October 2012; published online 9 December 2012; DOI: 10.1038/ncb2633

a

	Cell density (cell ml^{-1})	Live cell Plo1 Recruitment duration (min)	Fixed cell Plo1 1 dot : 2 dots	Fixed cell MPM2 1 dot : 2 dots
Wild type	1×10^6		1	1.1
cut12.s11			2.5	2.6
plo1.GFP		30.5 ± 15.5	1.1	1
cut12.s11 plo1.GFP		64.4 ± 26.9	2.4	2.5
Wild type	2×10^6		1.3	1.4
plo1.GFP		36.3 ± 20.2	1.4	1.3
Wild type	4×10^6		1.8	1.7
plo1.GFP		41.8 ± 21	1.8	1.8

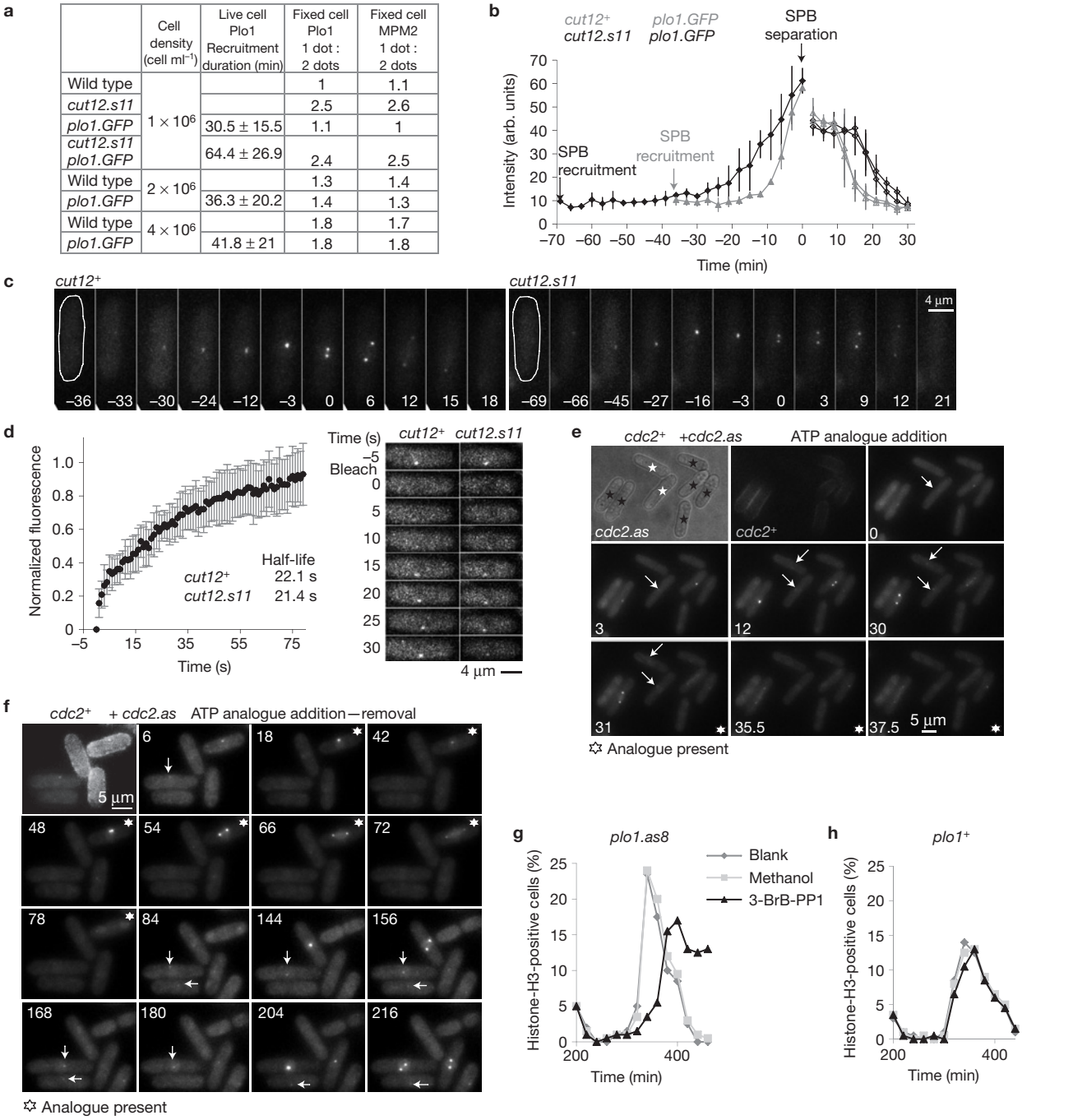

Figure 1 MPF activity controls Plo1.GFP recruitment to the SPB in late G2 phase. (**a**) Timing of Plo1.GFP recruitment before SPB separation (living cells) and the ratios of 1 dot (G2, early mitotic SPB) to two dots (mitotic SPB) for MPM2 staining. (**b**) Plots of the intensity of the Plo1.GFP signals averaged for three cells. The single plot for each strain splits into two different plots after SPB separation to indicate the signals arising from two individual SPBs that emerge from this single focus of paired SPB signals in G2. intensity of the two (see also Supplementary Video S1). (**c**) Time-lapse images of *plo1.GFP* and *cut12.s11 plo1.GFP* cells. (**d**) FRAP of the signal from a late G2 Plo1.GFP SPB in wild-type cells (left). The FRAP profile of a *cut12.s11 plo1.GFP* strain was indistinguishable from this wild-type plot (right; see also Supplementary Video S2). (**e**,**f**) Wild-type (TRITC–lectin pre-treated) and analogue-sensitive (*cdc2.as*) cells (no coating) recorded side by side in the same field of view at 25 °C. The timing of the addition of 25 µM 1NA-PP1 is indicated in the panel. Control *cdc2*$^+$ cells advanced through mitosis irrespective of the presence of analogue with Plo1.GFP on their SPBs whereas Plo1.GFP signal left the SPBs of neighbouring *cdc2.as* mutant cells following analogue addition. White arrows indicate Plo1.GFP signals on SPBs. See also Supplementary Videos S3 and S4. (**g**,**h**) Size-selected cultures of either *plo1.as8* (**g**) or *plo1*$^+$ (**h**) cells were split into three following completion of the first synchronous division after size selection and treated as indicated in the legend to the graphs before processing for immunofluorescence microscopy with phospho-histone H3 Ser 10 antibodies. The analogue 3-BrB-PP1 was added to a final concentration of 20 µM. The numbers in time-lapse images indicate minutes.

cell cycles. In strains harbouring the *plo1.as1, plo1.as2, plo1.as3* or *plo1.as4* mutations that are predicted to confer sensitivity[13], addition of analogue had little impact on the most sensitive readout of Plo1 function, spindle formation[14]. However, septation was compromised in the first division after the addition of 40 μM 3MB-PP1 to *plo1.as3* cells (data not shown), indicating a modest degree of sensitization[14]. We therefore studied the structure of AMP-PNP-bound human Plk1 (ref. 15) to seek notable differences between the structure of this mammalian kinase that can be sensitized to ATP analogue inhibition and its refractory fission yeast counterpart, Plo1. Plk1 harbours a phenylalanine at position 170 at the bottom of the ATP-binding pocket that is replaced by methionine in Plo1. Mutation of this methionine to phenylalanine in a *plo1.as3* backbone created the *plo1.as8* allele that responded to 3MB-PP1 or 3-BrB-PP1 addition by arresting mitotic progression with the monopolar spindle phenotype that is a characteristic of severely compromised Plo1 function[14] (Supplementary Fig. S1a,b). Addition of 20 μM 3-BrB-PP1 to G2 *plo1.as8* cells delayed the phosphorylation of histone H3 Ser 10 that accompanies mitotic commitment by 40 min (Fig. 1g,h).

Plo1 comprises a catalytic domain and two polo boxes that direct the kinase to target molecules that are either direct substrates or platforms from which neighbouring substrates can be phosphorylated[16–18] (Supplementary Fig. S1c). We reasoned that Plo1 could be directed to a site of choice by replacement of the polo boxes with a surrogate targeting sequence. We replaced the polo box domain of *plo1.as8* with sequences encoding the GFP-binding protein[19–21] (GBP), in a transgene that was expressed from an ectopic location. We incorporated mutations conferring constitutive activation[8] into the catalytic domain of this hybrid molecule to override the controls that normally coordinate Plo1 activity with cell-cycle progression (Supplementary Fig. S1c). Ectopic expression of this Plo1.RL chimaera in the presence of inhibitory ATP analogue targets a restrained kinase to any location that hosts GFP (Supplementary Fig. S2a). Subsequent analogue removal releases sustained Plo1 kinase activity at the target site. This approach enabled us to uncouple kinase activation from its normal cell-cycle context and to examine which events are triggered by forced Plo1 activation at a particular location.

Plo1.RL activation at SPBs through recruitment to Cut12.NEGFP promoted mitotic commitment (Fig. 2a). A lower level of mitotic induction arose from recruitment to the SPB components Pcp1.GFP and Sid4.GFP whereas none followed targeting to any other location (Fig. 2a and Supplementary Fig. S2b). Bleaching the fluorescence signal derived from either the host molecule Cut12.NEGFP or the associated Plo1.RLTom chimaeric kinase revealed no turnover of the Cut12.NEGFP/Plo1.RLTom complex at SPBs (Fig. 2b). We therefore investigated whether the anchored Plo1.RL chimaeric kinase relied on the endogenous, mobile, Plo1 to promote mitotic commitment. *plo1.ts41* cells (Supplementary Fig. S1e,f) harbouring Cut12.NEGFP-anchored Plo1.RL were shifted from 25 °C to 36 °C to inhibit Plo1 function as the inhibitory analogue was removed. Different induction times produced different levels of Plo1.RL at this point of release. Levels of Plo1.RL (18 or 20 h induction) that were competent to induce mitosis when the endogenous Plo1 kinase was a functional wild-type molecule were unable to do so when it was the incapacitated Plo1.ts41 (Fig. 2c).

As MPF associates with G2 SPBs (refs 22,23) and controls SPB recruitment of Plo1 (Fig. 1e,f), we investigated whether it was also responsible for generating the pro-mitotic Plo1 signal at SPBs. We examined this possibility with a Cdc2–GBP fusion protein, Cdc2.RL (*cdc2.F84GY15F*, Supplementary Fig. S1c) that is insensitive to inhibition by either Mik1 or Wee1 (ref. 24) and sensitive to ATP analogues[11]. Activation of Cdc2.RL by analogue removal from strains in which the chimaeric kinase had been recruited to a variety of locations (Supplementary Fig. S3a) mirrored the Plo1.RL data: SPB recruitment through Cut12.NEGFP gave a strong induction of mitosis; weaker levels followed SPB recruitment with either Pcp1.GFP or Sid4.GFP and no induction was seen following recruitment to any other location (Fig. 2d and Supplementary Fig. S3b). Bleaching Cut12.NEGFP-anchored Cdc2.RLTom revealed a static association with the SPBs (Supplementary Fig. S3c). MPM2 reactivity of SPBs showed that the wave of mitosis that arose from activation of Cut12.NEGFP-anchored Cdc2.RL was preceded by Plo1 activation (Supplementary Fig. S3d). Consistently, this ability of Cut12.NEGFP-anchored Cdc2.RL to induce mitosis relied on Plo1 activity (Fig. 2e).

Three further Cut12.NEGFP/Cdc2.RL experiments were informative. When the *cdc2* encoding sequence retained Tyr 15 (Cdc2.RLY15, Supplementary Fig. S1c), mitosis was not induced (Fig. 2f), indicating that the balance of Wee1 and Cdc25 activities normally determines the timing at which SPB-bound MPF activity is enhanced to trigger mitosis. Mitotic induction by SPB-tethered Cdc2-RL was blocked in a *cdc2.33* background in which the bulk population of MPF within the nucleus[22,23] was inactivated (Fig. 2g,h), even though Plo1 activity was promoted on the SPBs of these interphase cells (Fig. 2i). Thus, division is not driven from the SPB, rather MPF activation at the SPB serves as a trigger event that promotes conversion of the bulk population MPF throughout the cell[22,23] to the active state. The second wave of mitosis after analogue removal was abolished by the inclusion of hydroxyurea in the replacement, analogue-free, medium (Fig. 2f), indicating that the checkpoint remains intact.

The point in G2 phase at which Plo1 was initially recruited to G2 SPBs is strongly influenced by cell density (Fig. 1a). Consistently, nutrient provision and TOR signalling is closely tied to SPB recruitment of Plo1 in mitotic control[25–28]. This context dependency is highly reminiscent of the way by which the timing of the G2 event NETO changes in response to changes in nutrient supply[3]. We therefore examined the relationship between Plo1 recruitment to the G2 SPB and NETO. Strikingly, the two events were coincident: in counts of 100 cells, every post-NETO G2 cell exhibited a Plo1.GFP signal at its SPB whereas neighbouring pre-NETO cells had none (Fig. 3a). The correlation between NETO and Plo1 recruitment was even maintained when Plo1 SPB recruitment was advanced by 30 min by *cut12.s11* (Fig. 3b).

To determine whether there was a direct causal relationship between Plo1 activity and NETO, NETO was monitored when small G2 *plo1.ts41* cells (Supplementary Fig. S1e,f) were shifted from 25 °C to 36 °C. NETO execution was severely compromised by Plo1 inactivation (Fig. 3c and Supplementary Fig. S1g). To determine whether it was the SPB-associated pool of Plo1 that triggered NETO, we targeted Plo1.RL to various locations in *cdc10.v50* cells. At 36 °C, *cdc10.v50* arrests cell-cycle progression in G1 phase before NETO (ref. 3). NETO was triggered when Plo1.RL was activated at the SPBs of *cdc10.v50* cells but nowhere else, including recruitment to the cell end itself through either Tea1.v5GFP or For3.GFP fusion proteins (Fig. 3d and Supplementary Fig. S2a).

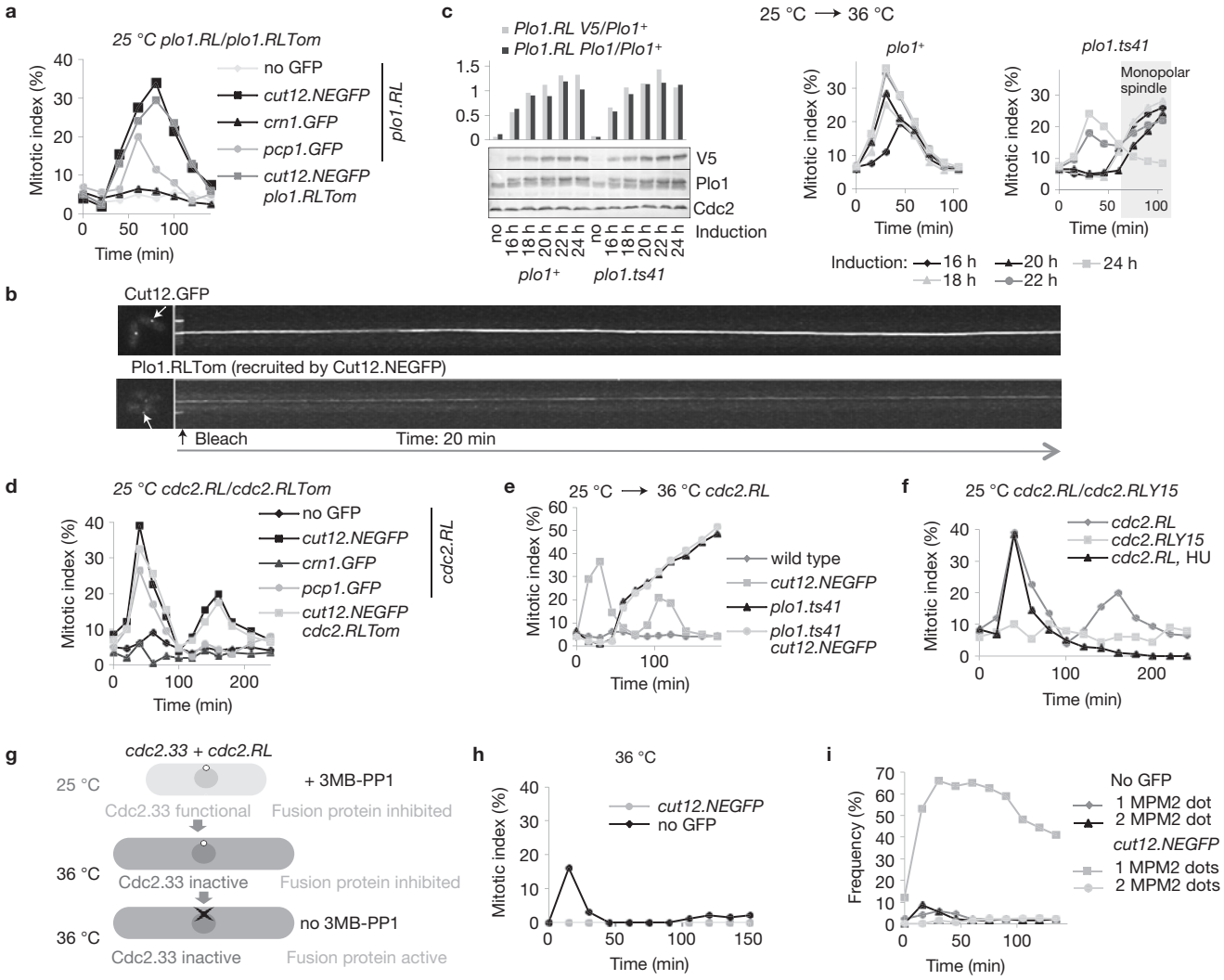

Figure 2 Ectopic activation of either Plo1 or MPF on G2 SPBs promotes mitotic commitment. (**a**) 3-MB-PP1 removal from strains hosting a de-repressed *plo1.RL* allele (see also Supplementary Fig. S2b). *crn1*$^{+}$encodes the actin-binding protein coronin; *pcp1*$^{+}$ encodes pericentrin. (**b**) Photobleaching of Cut12.NEGFP and Cut12.NEGFP-anchored Plo1.RLTom. (**c**) Left panel: expression of *plo1.RL* was induced in *cut12.NEGFP plo1*$^{+}$ or *cut12.NEGFP plo1.ts41* backgrounds by removal of thiamine at $t = 0$. Levels of the endogenous and chimaeric Plo1 molecules were assessed by Plo1 polyclonal antibodies and V5 monoclonal antibodies detected Plo1.RL alone. Graphs on the right: cells were shifted from 25 °C to 36 °C at $t = 0$ immediately after filtration into analogue-free medium. Tubulin immunofluorescence revealed the mitotic index. (**d**) 3-MB-PP1 removal from strains hosting a de-repressed *cdc2.RL* allele (for recruitment to other locations, see Supplementary Fig. S3b). (**e**) 3-MB-PP1 removal from *cdc2.RL*-expressing strains indicated that MPF activation relied on Plo1 function to drive mitotic commitment. The accumulation of mitotic *plo1.ts41* cells from 60 min reflected the block to mitotic progression that arose from Plo1 inactivation (Supplementary Fig. S1e,f). (**f**) 3-MB-PP1 removal from *cut12.NEGFP* strains hosting either a de-repressed *cdc2.RL* or *cdc2.RLY15* chimaera. For *cdc2.RL* HU the analogue-free medium that was substituted at $t = 0$ to release the kinase activity contained 10 mM hydroxyurea (HU) to block DNA synthesis. (**g**) A schematic diagram depicting the scheme used to generate the mitotic index (**h**) and MPM2 staining data in **i**. (**h**) MPF activation through *cdc2.RL* expression and analogue release promoted a modest level of mitotic commitment in *cdc2.33* cells at 36 °C when it was free to diffuse throughout the cell (*cut12*$^{+}$), but not when restricted to the SPB (*cut12.NEGFP*). (**i**) MPM2 staining demonstrating that MPF activation on *cdc2.33* SPBs at 36 °C triggered Plo1 activation on SPBs even though cells did not enter mitosis.

The observation that G2-arrested *cdc2.33* cells undergo NETO (ref. 3), yet NETO can be triggered by Plo1 activation on SPBs (an MPF-dependent event; Fig. 1e–f), prompted us to re-examine the relationship between NETO and Cdc2 with the *cdc2.as* allele. Addition of 1 μM BrB-PP1 to G2 *cdc2.as* cells mimicked temperature-mediated inactivation of *cdc2.33* in having no impact on NETO yet arresting cell-cycle progression in G2. However, a stronger level of inhibition (20 μM BrB-PP1) did block NETO (Fig. 4a and Supplementary Fig. S4), indicating that the threshold of MPF activity required for NETO was lower than that for mitotic commitment.

The contribution of SPB-associated MPF to the promotion of NETO cannot be assessed by the Cdc2.RL approach in wild-type cultures because the immediate induction of mitotic commitment (Fig. 2d) obscures any impact on NETO. We therefore blocked the propagation of the mitotic commitment signal with the *cdc2.33* mutation (Fig. 2h) before assessing NETO induction. Hydroxyurea

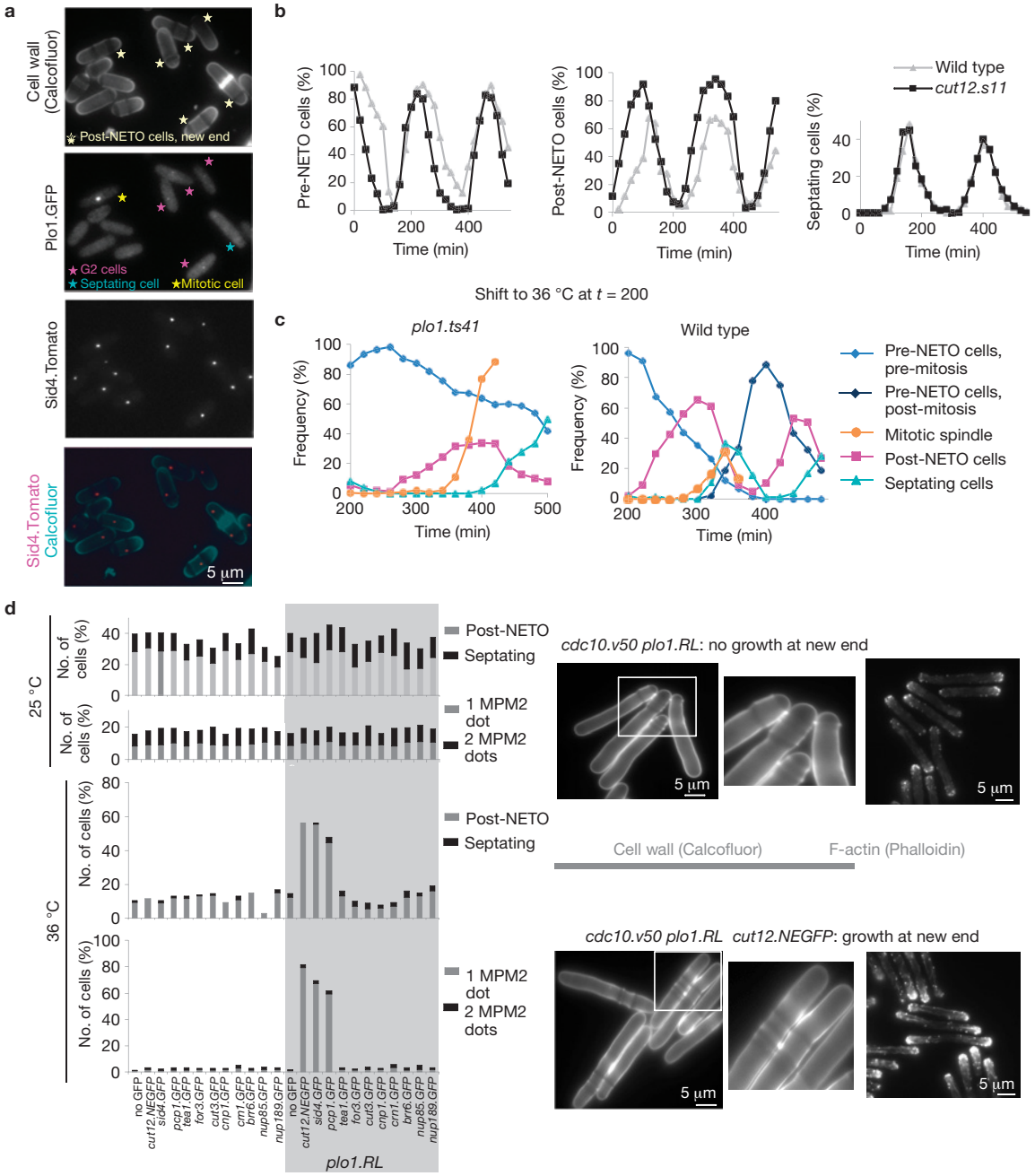

Figure 3 NETO is triggered by Plo1 activation/recruitment on the G2 SPB. (**a**) Fluorescence imaging of cell wall signals (calcofluor, top), Plo1.GFP and Sid4.Tom of living cells of the indicated strains. Arrows identify cells with Plo1.GFP signals on SPBs. (**b**) Size-selected small G2 cells were fixed and scored for NETO status and septation index as they transited the cell division cycle. (**c**) Cultures in which cell-cycle progression had been synchronized by the selection of small cells at $t = 0$ were allowed to transit one cell cycle (Supplementary Fig. S1g) before the temperature was shifted to 36 °C and the frequency of NETO and the mitotic spindle index were scored in fixed cells. As indicated in Fig. 1g, inactivation of Plo1 delayed mitotic commitment in the *plo1.ts41* panel. Despite this delay, over 60% of cells failed to undergo NETO by the time the mitotic index rose sharply as cells accumulate with monopolar spindles (Supplementary Fig. S1f). (**d**) Mutants harbouring *cdc10.v50* and the indicated GFP fusion genes were grown to early log phase at 25 °C before the *plo1.RL* allele was induced by removal of thiamine in the presence of 40 μM 3MB-PP1. After dilution and a further 24 h at 25 °C the early log phase cells were filtered into analogue- and thiamine-free medium and split into two, one half being kept at 25 °C (upper), the other being shifted to 36 °C (lower). Five hours later, the cells were fixed and the frequency of NETO was scored (left). The panels on the right show examples of the wild-type control (upper) and *cut12.NEGFP* (lower) *cdc10.v50* strains after incubation at 36 °C stained with calcofluor to highlight cell wall material or TRITC phalloidin to stain F-actin.

treatment enriched the pool of S-phase-arrested (pre-NETO; ref. 3) cells before temperature shift from 25 °C to 36 °C for 1 h to inactivate Cdc2.33 before analogue removal activated the SPB-associated Cdc2.RL (Fig. 4b). NETO was triggered by Cdc2.RL activation on the SPB, but at no other location. Recruitment to Cut12 had a greater impact than to Pcp1 or Sid4 (Fig. 4c and Supplementary Fig. S3e). Critically, this

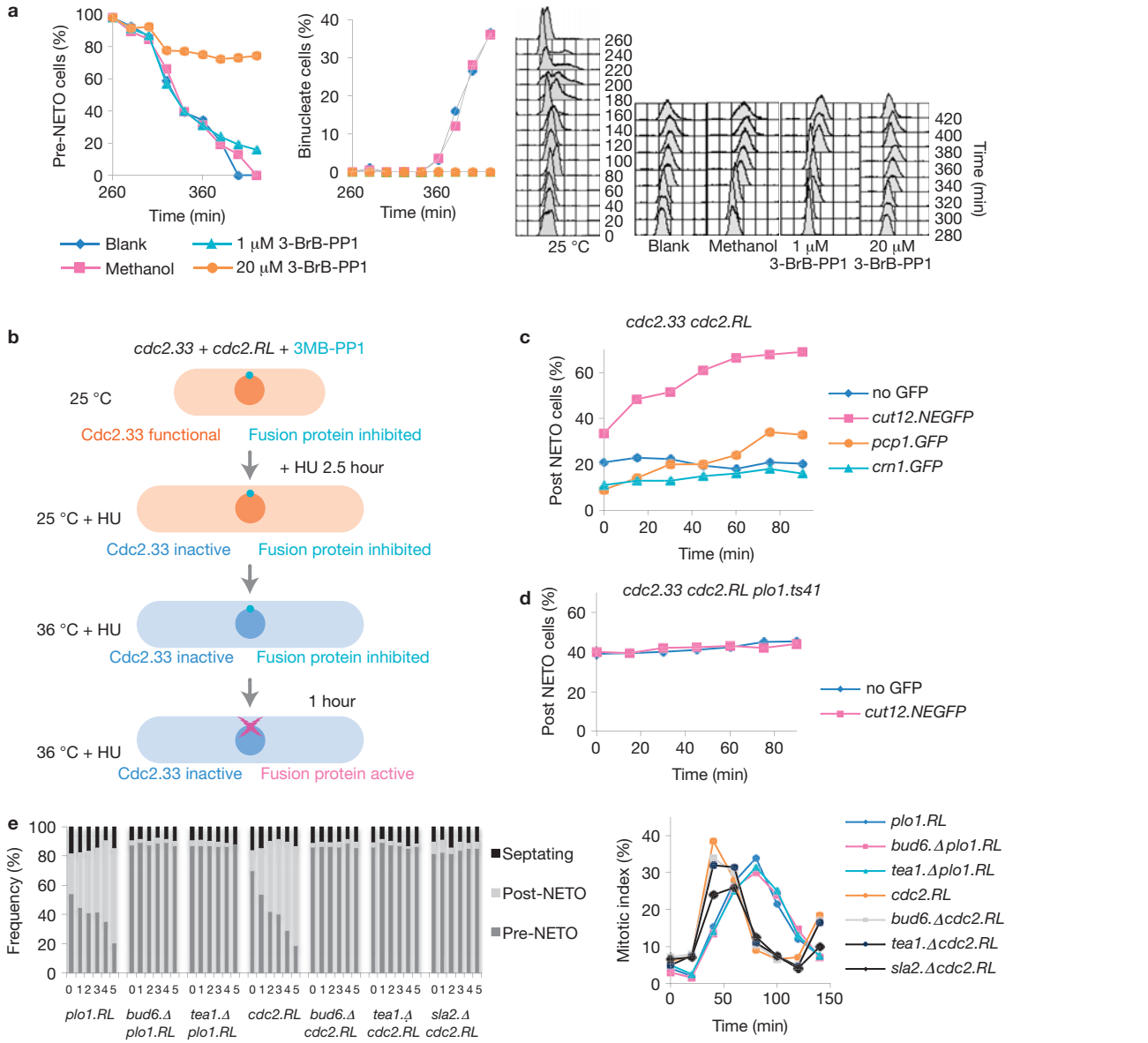

Figure 4 MPF activation on the SPB triggers NETO in a Plo1-dependent manner. (**a**) Cell-cycle progression was synchronized by the selection of small, G2, *cdc2.as* cells at 25 °C. After transit of one cell cycle at 25 °C (Supplementary Fig. S4a) the culture was split into four equal aliquots that were all shifted to 32 °C. Either 1 or 20 μM 3-BrB-PP1, solvent alone or nothing was added before NETO was scored in fixed samples at the indicated intervals. Samples were also processed for FACS (fluorescence-activated cell sorting) analysis to monitor DNA content (right). For a repeat of this FACs analysis see Supplementary Fig. S4c. (**b**) The scheme used to assess whether analogue removal from strains harbouring *cdc2.RL* and the indicated GFP targeting proteins was able to induce NETO when the bulk population of MPF in the cell was inactivated by incubation of *cdc2.33* cells at 36 °C. HU, hydroxyurea. (**c**,**d**) Whereas NETO was induced when Cdc2.RL was targeted to the SPB by Cut12.NEGFP (**c**), no induction occurred when Plo1 kinase was inhibited (**d**). (**e**) Left, *cut12.NEGFP* cells containing the indicated additional mutations were treated as for Fig. 3d except that cells were maintained at 25 °C throughout. The time interval is in hours. Activation of Plo1 or Cdc2 on the SPB did not induce NETO in the polarity mutants *bud6.*Δ, *tea1.*Δ or *sla2.*Δ despite the fact that processing of the *cut12.NEGFP* mutant strains as described for Fig. 2a revealed that none of them compromised the ability of activation of either kinase on SPBs to induce mitosis (right).

ability of Cut12.NEGFP-anchored Cdc2.RL to induce NETO was reliant on Plo1 activity (Fig. 4d). It also required the polarity factors Tea1, Bud6 and Sla2 (Fig. 4e).

We propose that Plo1 recruitment to SPBs in G2 phase both triggers the cell-cycle-dependent morphogenetic switch to bipolar growth and constitutes a priming event that licenses the cell to regulate the timing of mitotic commitment. The MPF dependency and activity of the Plo1 recruited to these G2 SPBs suggests a local activation of the feedback loops that will later be employed at remote locations to drive the global cell cycle during mitotic commitment (Fig. 5a). As NETO happens as soon as the feedback loop is running on the SPB the target/s for Plo1 in NETO control probably differ from those in G2/M commitment control. The fact that it is only constitutively active forms of MPF that can override the normal controls to induce mitosis and NETO

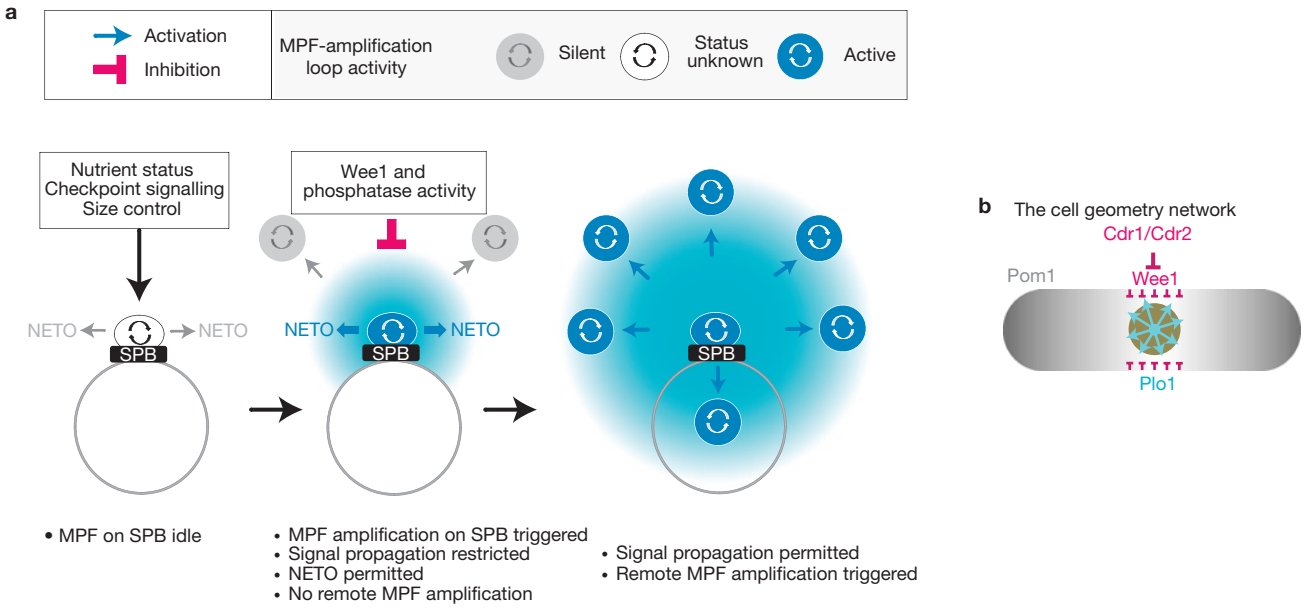

Figure 5 Model of feedback loop activation on the SPB and its subsequent propagation throughout the cell to promote mitotic commitment. (**a**) The absence of a readout for MPF activity on the SPB in early G2 means that it is not possible to propose activity at this site before activation/enhancement promotes Plo1 turnover in late G2 (left). MPF feedback loop enhancement/activation on the G2 SPB subsequently triggers the pathway that ultimately leads to NETO, yet this level of G2 activation is insufficient to trigger mitotic commitment (centre). Mitosis is triggered later when there has either been a reduction in the level of inhibition by Wee1 or phosphatases such as PP2A and the Cdc14 homologue Flp1/Clp1 or feedback loop activity is enhanced to exceed an inhibitory threshold, or a combination of the two (right). It is likely that the different pathways that impact on the timing of mitotic commitment will target different parts of this switch. (**b**) The spatial organization of Plo1 activation on the SPB relative to the Pom1/Cdr1/Cdr2 pathway that couples tip extension to mitotic commitment[29,30]. Note that the close relationship between the position of the Cdr1/Cdr2/Wee1 nodes and the position of the nucleus that is established by the cycles of nuclear import/export of Mid1 places this inhibitory network directly over the SPB, putting it in the optimal location to dampen/neuter the pro-mitotic signal emerging from the SPB.

when targeted to the SPB (Fig. 2f and Supplementary Figs S2d,e and S3f) indicates that Wee1 activity blocks the propagation of the mitotic commitment signal from the SPB.

Once the restraining activity of Wee1 is removed/overcome, cells can execute mitosis. Given the relative location of the different signalling components, it would seem likely that the anti-mitotic activity of the equatorial belt of inhibitory nodes that contain Cdr1, Cdr2 and Wee1 and encircle the nucleus blocks the propagation of the signals emanating from the SPB (Fig. 5b)[29,30].

The well-documented ability of TOR signalling to influence the timing of mitotic commitment in fission yeast relies on its ability to promote Plo1 recruitment to the SPB (refs 25–28), indicating that, in some situations, enhancing the level of Plo1 signalling from the SPB is sufficient to advance the timing of mitotic commitment. Perhaps mitotic commitment is also finally triggered when Plo1 activity exceeds a critical threshold in unperturbed cell cycles.

As NETO ensures that each daughter cell will receive an experienced, old, cell tip that will be optimal for growth in the subsequent cell cycle, Plo1 recruitment to G2 SPBs could be seen as the first phase of mitotic commitment. However, the question remains as to how a signal that emanates from the cell equator triggers an event at the cell extremity (NETO). A recent study may hold the clue[31]. The Cdc42 activation that drives tip growth is not a persistent signal at one end. Rather, it alternates between the two cell tips throughout interphase. Thus, Cdc42 is activated at new ends every 3 min throughout early G2 up to NETO. However, NETO is triggered only once global Cdc42 activity exceeds a critical threshold level of global Cdc42 activation. A general signal emanating from the SPB could set the level of this general threshold by targeting Cdc42 or its regulators globally.

Given the impact of TOR and stress pathways on SPB recruitment of Plo1 (refs 26,27,32) and the coordination of cytokinetic ring formation and function by a second cell-cycle regulatory network on the same SPBs (the septum initiation network[33]), we propose that the SPB (and by implication the centrosome) acts as a platform at which signals from diverse signalling pathways are integrated to generate coordinated and coherent signals to control cell-cycle progression. □

METHODS

Methods and any associated references are available in the online version of the paper.

Note: Supplementary Information is available in the online version of the paper

ACKNOWLEDGEMENTS

We thank B. Hodgson for technical assistance; V. Doye (Insitut Jacques Monod, Paris, France), D. Mulvihill (University of Kent, UK), U. Fleig (Düsseldorf, Germany) and D. Feret (Paterson Institute, UK) for strains; K. Gull (Oxford University, UK) and H. Ohkura (Edinburgh University, UK) for antibodies; D. Feret (Paterson Institute, UK), G. Pereira (DKFZ, Germany) and A. Carr (GDSC, Sussex, UK) for plasmids; and D. Bitton (Paterson Institute, UK) for discussions during the design of *plo1.as8*. This work was supported by Cancer Research UK (CRUK) grant number C147/A6058. V.S. and A.K. were supported by the Swiss National Science Foundation and EPFL.

AUTHOR CONTRIBUTIONS

I.M.H. conceived the study. A.K. and V.S. generated *cdc2.as*. A.P. generated the conditional polo kinase alleles, including Plo1.RL. V.A.T. and K.Y.C. carried out the imaging work in Fig. 1. A.G. performed the remainder of the experiments with occasional assistance from A.P. and K.Y.C. for more complex experiments and cloning. I.M.H. wrote the manuscript with input and discussions from all authors.

COMPETING FINANCIAL INTERESTS

The authors declare no competing financial interests.

Published online at www.nature.com/doifinder/10.1038/ncb2633
Reprints and permissions information is available online at www.nature.com/reprints

1. Nurse, P. Universal control mechanism regulating onset of M-phase. *Nature* **344,** 503–508 (1990).
2. Jackman, M., Lindon, C., Nigg, E. A. & Pines, J. Active cyclin B1-Cdk1 first appears on centrosomes in prophase. *Nat. Cell Biol.* **5,** 143–148 (2003).
3. Mitchison, J. M. & Nurse, P. Growth in cell length in the fission yeast *Schizosaccharomyces pombe*. *J. Cell Sci.* **75,** 357–376 (1985).
4. Mulvihill, D. P., Petersen, J., Ohkura, H., Glover, D. M. & Hagan, I. M. Plo1 kinase recruitment to the spindle pole body and its role in cell division in *Schizosaccharomyces pombe*. *Mol. Biol. Cell* **10,** 2771–2785 (1999).
5. Hudson, J. D., Feilotter, H. & Young, P. G. *stf1*: non wee mutations epistatic to *cdc25* in the fission yeast *Schizosaccharomyces pombe*. *Genetics* **126,** 309–315 (1990).
6. Bridge, A. J., Morphew, M., Bartlett, R. & Hagan, I. M. The fission yeast SPB component Cut12 links bipolar spindle formation to mitotic control. *Genes Dev.* **12,** 927–942 (1998).
7. Tallada, V. A., Bridge, A. J., Emery, P. E. & Hagan, I. M. Suppression of the *S. pombe cut12.1* cell cycle defect by mutations in *cdc25* and genes involved in transcriptional and translational control. *Genetics* **176,** 73–83 (2007).
8. MacIver, F. H., Tanaka, K., Robertson, A. M. & Hagan, I. M. Physical and functional interactions between polo kinase and the spindle pole component Cut12 regulate mitotic commitment in *S. pombe*. *Genes Dev.* **17,** 1507–1523 (2003).
9. Tanaka, K. *et al*. The role of Plo1 kinase in mitotic commitment and septation in *Schizosaccharomyces pombe*. *EMBO J.* **20,** 1259–1270 (2001).
10. Bähler, J. *et al*. Role of polo kinase and Mid1p in determining the site of cell division in fission yeast. *J. Cell Biol.* **143,** 1603–1616 (1998).
11. Dischinger, S., Krapp, A., Xie, L., Paulson, J. R. & Simanis, V. Chemical genetic analysis of the regulatory role of Cdc2p in the S. pombe septation initiation network. *J. Cell Sci.* **121,** 843–853 (2008).
12. May, J. & Mitchison, J. M. Length growth in fission yeast cells measured by two novel techniques. *Nature* **322,** 752–754 (1986).
13. Zhang, C. *et al*. A second-site suppressor strategy for chemical genetic analysis of diverse protein kinases. *Nat. Methods* **2,** 435–441 (2005).
14. Ohkura, H., Hagan, I. M. & Glover, D. M. The conserved *Schizosaccharomyces pombe* kinase Plo1, required to form a bipolar spindle, the actin ring, and septum, can drive septum formation in G1 and G2 cells. *Genes Dev.* **9,** 1059–1073 (1995).
15. Kothe, M. *et al*. Structure of the catalytic domain of human polo-like kinase 1. *Biochemistry* **46,** 5960–5971 (2007).
16. May, K. M., Reynolds, N., Cullen, F., Yanagida, M. & Ohkura, H. Polo boxes and Cut23 (Apc8) mediate an interaction between polo kinase and the anaphase-promoting complex for fission yeast. *J. Cell Biol.* **156,** 23–28 (2002).
17. Archambault, V. & Glover, D. M. Polo-like kinases: conservation and divergence in their functions and regulation. *Nat. Rev. Mol. Cell Biol.* **10,** 265–275 (2009).
18. Elia, A. E., Cantley, L. C. & Yaffe, M. B. Proteomic screen finds pSer/pThr-binding domain localizing Plk1 to mitotic substrates. *Science* **299,** 1228–231 (2003).
19. Rothbauer, U. *et al*. Targeting and tracing antigens in live cells with fluorescent nanobodies. *Nat. Methods* **3,** 887–889 (2006).
20. Rothbauer, U. *et al*. A versatile nanotrap for biochemical and functional studies with fluorescent fusion proteins. *Mol. Cell Prot.: MCP* **7,** 282–289 (2008).
21. Bertazzi, D. T., Kurtulmus, B. & Pereira, G. The cortical protein Lte1 promotes mitotic exit by inhibiting the spindle position checkpoint kinase Kin4. *J. Cell Biol.* **193,** 1033–1048 (2011).
22. Alfa, C. E., Ducommun, B., Beach, D. & Hyams, J. S. Distinct nuclear and spindle pole body populations of cyclin-cdc2 in fission yeast. *Nature* **347,** 680–682 (1990).
23. Decottingnies, A., Zarzov, P. & Nurse, P. *In vivo* localisation of fission yeast cyclin-dependent kinase cdc2p and cyclin B cdc13p during mitosis and meiosis. *J. Cell Sci.* **114,** 2627–2640 (2001).
24. Gould, K. L. & Nurse, P. Tyrosine phosphorylation of the fission yeast Cdc2+ protein-kinase regulates entry into mitosis. *Nature* **342,** 39–45 (1989).
25. Petersen, J. & Nurse, P. TOR signalling regulates mitotic commitment through the stress MAP kinase pathway and the Polo and Cdc2 kinases. *Nat. Cell Biol.* **9,** 1263–1272 (2007).
26. Halova, L. & Petersen, J. Aurora promotes cell division during recovery from TOR-mediated cell cycle arrest by driving spindle pole body recruitment of Polo. *J. Cell Sci.* **124,** 3441–3449 (2011).
27. Petersen, J. & Hagan, I. M. Polo kinase links the stress pathway to cell cycle control and tip growth in fission yeast. *Nature* **435,** 507–512 (2005).
28. Hartmuth, S. & Petersen, J. Fission yeast Tor1 functions as part of TORC1 to control mitotic entry through the stress MAPK pathway following nutrient stress. *J. Cell Sci.* **122,** 1737–1746 (2009).
29. Moseley, J. B., Mayeux, A., Paoletti, A. & Nurse, P. A spatial gradient coordinates cell size and mitotic entry in fission yeast. *Nature* **459,** 857–860 (2009).
30. Martin, S. G. & Berthelot-Grosjean, M. Polar gradients of the DYRK-family kinase Pom1 couple cell length with the cell cycle. *Nature* **459,** 852–856 (2009).
31. Das, M. *et al*. Oscillatory dynamics of Cdc42 GTPase in the control of polarized growth. *Science* **337,** 239–243 (2012).
32. Petersen, J. TOR signalling regulates mitotic commitment through stress-activated MAPK and Polo kinase in response to nutrient stress. *Biochem. Soc. Trans.* **37,** 273–277 (2009).
33. Simanis, V. Events at the end of mitosis in the budding and fission yeasts. *J. Cell Sci.* **116,** 4263–4275 (2003).

DOI: 10.1038/ncb2633

METHODS

Cell culture and growth. Strains used in this study are listed in Supplementary Table S1. Cells were grown and maintained according to ref. 34. Appropriately supplemented EMM2 synthetic medium was used for all experiments. As cell density alters the nutritional environment of the cell, which, in turn, influences the timing of Plo1 recruitment to the SPB (Fig. 1a), all measurements of Plo1.GFP recruitment were conducted with prototrophs in filter-sterilized supplemented EMM2 at 25 °C. Centrifugal elutriation was used to isolate small G2 cells[35]. All such synchronized cultures were diluted to a concentration of 1×10^6 cells ml^{-1} after elutriation. ATP analogues[36] (Toronto Research Chemicals, Dalton Pharma Services) were dissolved in methanol to generate 50 mM stock solutions that were subsequently added to cultures. Removal of analogue from the cell environment was achieved by filtration of the cells from culture followed by re-suspension in an identical volume of pre-warmed analogue-free medium.

Microscopy/FACS analysis. Tubulin, Sad1, MPM2 and anti-histone H3 phospho-Ser 10 immunofluorescence and calcofluor or phalloidin staining were conducted using established procedures[3,8,37–39]. Affinity-purified polyclonal Sad1 antibodies[37] were used at a concentration of 1 in 25 and the dilution of tissue culture supernatant containing the TAT1 monoclonal antibody[40] (gift from K. Gull, University of Oxford) was 1 in 80. Antibodies that recognized histone H3 when phosphorylated on Ser 10 were generated and affinity purified by Eurogentec and used at a concentration of 1 in 100. MPM2 antibody (Upstate 05-368) that recognized a phospho-epitope on the SPB that is dependent on Plo1 phosphorylation[8,41] was used at a concentration of 1 in 100. For detection of the V5 epitope in Plo1.RL and Cdc2.RL molecules polyclonal antibodies against the epitope (Bethyl Laboratories A190-120A) were used at a concentration of 1 in 100 following fixation with 4% formaldehyde for either 10 (Cut12, Pcp1, Sid4, Cnp1) or 30 (Crn1, Cut3, Nup85, Nup189) minutes. Thirty minutes in 4% formaldehyde was also used to detect Plo1.RL in Tea1.GFP cells in which the presence of the SV5 epitope in the fusion protein forced us to detect the hybrid molecule with Plo1 polyclonal sera at a concentration of 1 in 100 (ref. 4). DNA content analysis through FACS used Cytox green (Invitrogen) according to published procedures[42].

Western blotting. Plo1 polyclonal antisera[43] were used at a concentration of 1 in 500. PN24 anti-Cdc2 polyclonal antisera were used at a concentration of 1 in 500 to detect Cdc2. Polyclonal antibodies against the SV5 epitope (V5) were used at a concentration of 1 in 500.

Live-cell imaging. All quantitative microscopy was conducted on a DeltaVision system (Applied Precision) fitted with a Zeiss ×100, 1.45 NA objective in conjunction with Softworx (Applied Precision) and Imaris (Bitplane) software. Cells were mounted in a Bioptechs FCS2 chamber. The images shown are maximal projections of 20 sections, with 0.3 μm between the slices; images were taken every 3 min. For the FRAP analysis images were taken every second. Qualitative assessment of analogue addition on Plo1.GFP recruitment in *cdc2.as* was conducted on either DeltaVision or on an Olympus/Photometrics spinning-disc confocal microscope with Metamorph software. Cells were mounted in glass-based culture plates (Iwaki 5826-024) and media exchanged by aspiration with a Pasteur pipette. A 532 nm 25 mW laser was used to bleach the red fluorescence signal of the Tomato constructs and a 488 nm 25 mW laser bleached the green fluorescence emanating from Plo1 and Cut12 GFP fusion proteins.

Genetic manipulation. *plo1.ts41* was generated as described previously[44] with the exception that screening for temperature-sensitive mutants was conducted at 32 °C rather than 36 °C. The *plo1.as8* allele incorporates the canonical as3 mutations[13] alongside a mutation of methionine to phenylalanine at position 170. This last change was selected because the crystal structure of human Plk1 AMPPNP (ref. 15) identified this residue as being a major difference between the established Plk1 structure (Plk1.as3 can be strongly inhibited by ATP analogues) and the predicted structure of Plo1 (Plo1.as3 is not strongly inhibited by ATP analogues; data not shown). *plo1.as8* was integrated at the native locus using the marker switch approach[44]. To create Plo1.RL, the S124D and T197D mutations that confer constitutive activation[8] were introduced into *plo1.as8*, and the polo box domain (position 502–608) was replaced with a GBP (refs 19–21)–SV5 epitope double tag, and integrated the resultant *plo1.RL* gene into the *leu1* locus under the control of the *nmt81* promoter. *cdc2.RL* and *cdc2.F84GY15F* were created by site-directed mutagenesis and tagged at their C termini with GBP–SV5 before each cassette was introduced into a non-transcribed region of chromosome 3 under the control of the *nmt81* promoter. To create cdc2.RLTom and Plo1.RLTom, an Nde1 fragment encoding a functional Tomato fluorescence unit (a dimer of two subunits) was inserted at the amino terminus of *cdc2.RL* and *plo1.RL*. All mutant alleles were generated by PCR amplification and QuikChange mutagenesis (Stratagene).

34. Moreno, S., Hayles, J. & Nurse, P. Regulation of $p34^{cdc2}$ protein-kinase during mitosis. *Cell* **58,** 361–372 (1989).
35. Creanor, J. & Mitchison, J. M. Reduction of perturbations in leucine incorporation in synchronous cultures of *Schizosaccharomyces pombe* made by elutriation. *J. Gen. Micro.* **112,** 385–388 (1979).
36. Cipak, L. *et al.* Generation of a set of conditional analog-sensitive alleles of essential protein kinases in the fission yeast *Schizosaccharomyces pombe*. *Cell Cycle* **10,** 3527–3532 (2011).
37. Hagan, I. & Yanagida, M. The product of the spindle formation gene $sad1^+$ associates with the fission yeast spindle pole body and is essential for viability. *J. Cell Biol.* **129,** 1033–1047 (1995).
38. Petersen, J., Paris, J., Willer, M., Philippe, M. & Hagan, I. M. The *S. pombe* aurora related kinase Ark1 associates with mitotic structures in a stage dependent manner and is required for chromosome segregation. *J. Cell Sci.* **114,** 4371–4384 (2001).
39. Marks, J. & Hyams, J. S. Localization of F-actin through the cell-division cycle of *Schizosaccharomyces pombe*. *E. J. Cell Biol.* **39,** 27–32 (1985).
40. Woods, A. *et al.* Definition of individual components within the cytoskeleton of *Trypanosoma brucei* by a library of monoclonal-antibodies. *J. Cell Sci.* **93,** 491–500 (1989).
41. Davis, F. M., Tsao, T. Y., Fowler, S. K. & Rao, P. N. Monoclonal antibodies to mitotic cells. *Proc. Natl Acad. Sci. USA* **80,** 2926–2930 (1983).
42. Knutsen, J. H. *et al.* Cell-cycle analysis of fission yeast cells by flow cytometry. *PloS ONE* **6,** e17175 (2011).
43. Simanis, V. & Nurse, P. The cell cycle control gene *cdc2+* of fission yeast encodes a protein kinase potentially regulated by phosphorylation. *Cell* **45,** 261–268 (1986).
44. MacIver, F. H., Glover, D. M. & Hagan, I. M. A 'marker switch' approach for targeted mutagenesis of genes in *Schizosaccharomyces pombe*. *Yeast* **20,** 587–594 (2003).

nature cell biology

DOI: 10.1038/ncb2633

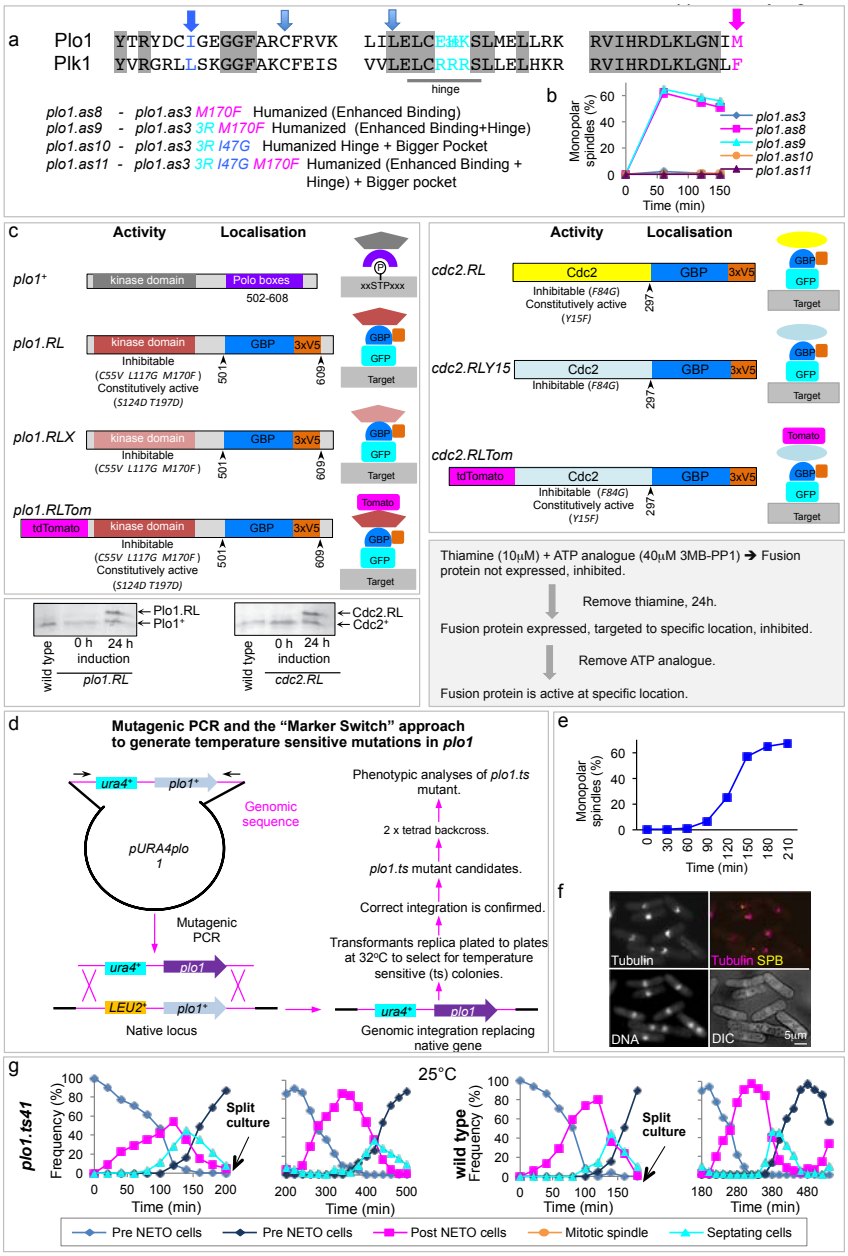

Figure S1 *plo1* mutants. a) Alignment of the sequences of human Plk1 and Plo1. Plk1 is rendered sensitive to ATP analogues by mutation of the gatekeeper and compensating residues predicted by Zhang et al.[28, 30] while the equivalent *plo1.as3* mutation displays only moderate analogue sensitivity (data not shown). The candidates for changes that might enhance the association with AMPPNP in the crystal structure of Plk1 are highlighted: The three arginine residues in the hinge region after the back of the ATP binding pocket that contains the gatekeeper residue (blue) and the phenylalanine at the bottom of the pocket (red). To make the pocket even larger isoleucine 47 was replaced by a smaller glycine. Below the alignment is a summary of the four mutations based on these changes that were introduced into the native *plo1* locus and assessed for impact on Plo1 function in response to analogue addition by monitoring the frequency of monopolar spindles in (b). c) The molecular structure of the *plo1* and *cdc2* alleles, their targeting specificities alongside the scheme used to induce the gene and subsequently activate the "caged" kinase by analogue removal. 3xV5 indicates three copies of the SV5 epitope. The level of Plo1.RL/Cdc2.RL attained in the 24 hour inductions used in all experiments were similar to those of the native kinases (with the exception of Figure 2c). (d) A cartoon of the approach used to generate a mutant library of temperature sensitive *plo1* alleles. The significant deviation from the approach taken previously to generate such conditional alleles[27] was setting the initial temperature for screening on plates to 32ºC, rather than 36ºC. Several highly penetrant mutants were identified following this simple modification. (e, f) Combined Sad1 and tubulin immunofluorescence was used to monitor the appearance of monopolar spindles following shift of an asynchronous *plo1.ts41* culture from the permissive temperature of 25ºC to the restrictive temperature of 36ºC at time 0 in the plot in d. f) Tubulin/Sad1/chromatin/DIC micrographs of cells at the 180 min in (d). g) Temperature mediated inactivation of Plo1 and NETO. Datasets from the experiments shown in Figure 3c. Small G2 cells were isolated from *plo1.ts41* (upper) or *plo1+* (lower) cultures at time 0. After completion of the first division each culture was split and one half shifted to 36ºC (Figure 3c) while the other was maintained at 25ºC (right panels). Calcofluor staining was used to score NETO and septation status.

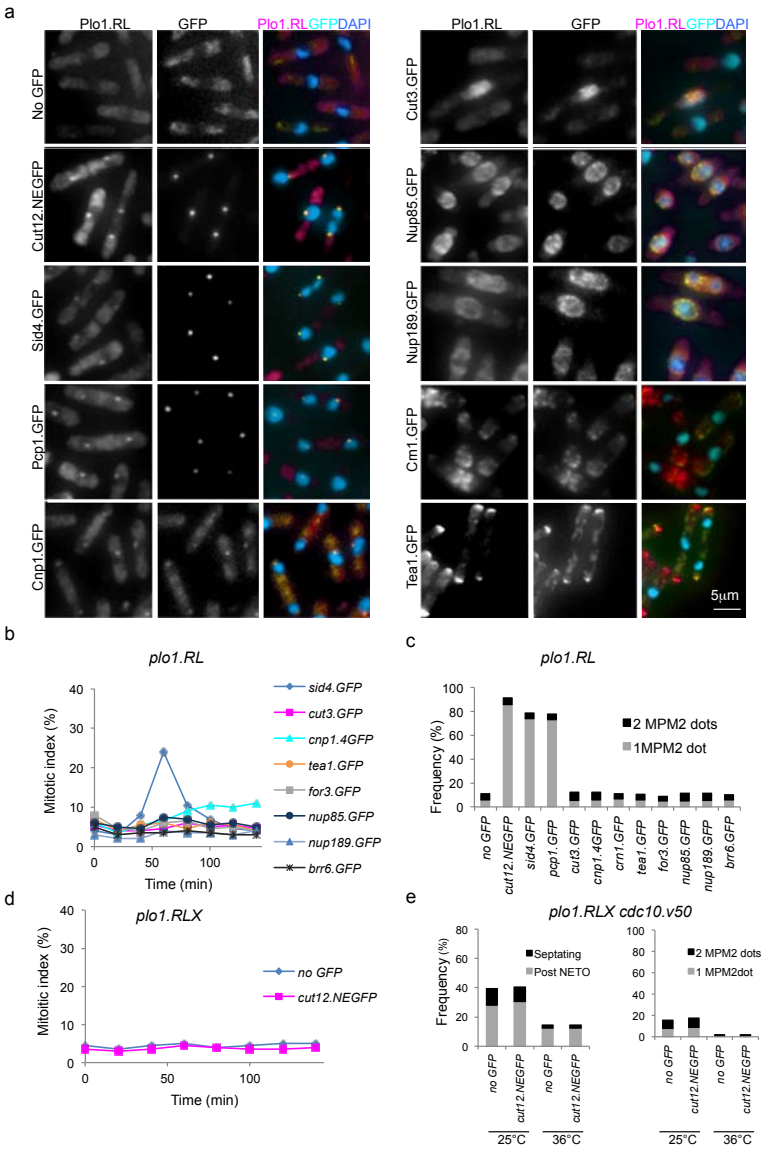

Figure S2 *plo1.RL* localization and impact upon mitotic control. a) Immunofluorescent localization of the Plo1.RL fusion protein (left panel) in cells harbouring different GFP fusion proteins (central panel (the signal is the endogenous fluorescence of GFP)). The overlap between the two signals can be seen in the false coloured merged image in the right hand panels. In all cases, with the exception of Tea1, the immunolocalisation of Plo1.RL in the left panel is via the detection of 3 SV5 epitopes that were inserted alongside the GBP sequences (Figure 2a). Polyclonal Plo1 antibodies were used to detect the Tea1.V5GFP fusion protein. *Key to target locations: sid4*$^{+}$ encodes a fission yeast restricted SPB component. *cut3*$^{+}$ encodes a condensin subunit. *cnp1*$^{+}$ encodes the centromeric histone H3 variant cenpA. *tea1*$^{+}$ encodes a encodes a kelch domain protein that is delivered to cell tips by microtubules where it regulates polarized cell growth. *for3*$^{+}$ encodes one of the three fission yeast members of the formin family of actin nucleating proteins. *nup85*$^{+}$ and *nup189*$^{+}$ encode nuclear core components. *brr6*$^{+}$ encodes a nuclear envelope protein that is recruited to the SPB during mitotic commitment to drive integration into the nuclear envelope at mitotic commitment and once more during mitotic exit to co-ordinate the expulsion from the envelope. b-e) Analogue (40μM 3MB-PP1) wash out experiments of the indicated strains as described for Figure 2a. (b) The moderate induction of mitosis following analogue washout in a sid4.GFP background was of a similar amplitude to that seen in pcp1.GFP background, while no induction was seen when Plo1.RL was recruited to any other location. Importantly, no induction was seen upon recruitment to Brr6 indicating that the timing of Plo1.RL recruitment to the SPB is critical. The increase in mitotic index in the cnp1.GFP background arose from compromised chromosome segregation as lagging chromosomes and chromosomes falling off spindles were frequently observed following analogue removal (data not shown). Similarly, cytokinesis was severely disrupted by analogue removal when Plo1.RL was recruited to the actin binding protein coronin (crn1.GFP (Figure 2a) data not shown). (c) MPM2 staining to monitor Plo1 activity at SPBs 20 minutes after analogue removal in the experiments shown in panel b and Figure 2a. Analogue removal clearly induced Plo1 activity on the G2/early mitotic SPBs (single dots). (d) Analogue wash out experiments of the indicated strains as described for Figure 2a with the exception that the plo1.RLX allele (Supplementary Figure 1c) that was used in these experiments lacked the S124D and T197D mutations that conferred constitutive activation (yet retained the analogue sensitizing mutations). No mitotic induction was observed, indicating that Plo1 activity at the SPB is normally subject to tight control to prevent premature mitotic commitment. (e) Calcofluor staining to monitor NETO state (left) and MPM2 staining to monitor Plo1 activity at SPBs (right) as described in Figure 3d. In stark contrast to the data with the constitutively active plo1.RL allele, analogue removal had no impact upon NETO or Plo1 activity on the G2/early mitotic SPBs (single dots) when the constitutive activation mutations were not present in the ectopically expressed chimera.

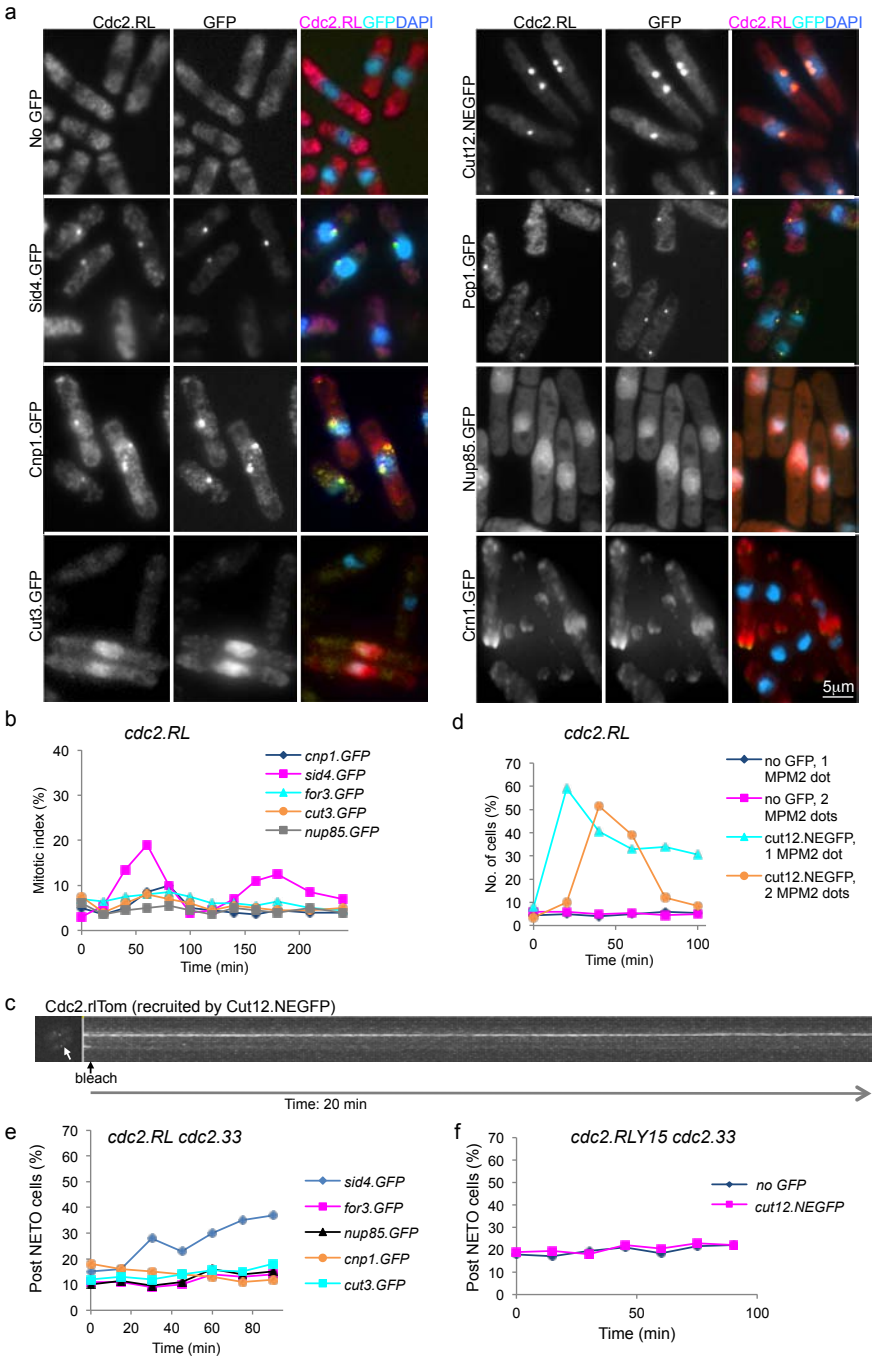

Figure S3 *cdc2.RL* localization and impact upon mitotic control. a) Immunofluorescent localization of the Cdc2.RL fusion protein (left panel) in cells harbouring different GFP fusion proteins (central panel (the signal is the endogenous fluorescence of GFP)). The overlap between the two signals can be seen in the false coloured merged image in the right hand panels. Immunolocalisation of Cdc2.RL is via the detection of the 3 V5 epitopes that had been fused to the end of the GBP sequences (Supplementary Figure 1c). b) Analogue wash out experiments of the indicated strains scoring the frequency of mitotic commitment as described for Figure 2b, e. (c) Photobleaching of Cdc2.RLTom anchored Cut12.NEGFP reveals stable associations with the SPB. (d) MPM2 staining to monitor Plo1 activity at SPBs after analogue removal in the experiments shown in Figure 2b. 1 MPM2 dot represents Plo1 activity on the single SPB foci of late G2/early mitotic cells, while 2 MPM2 dots arise from staining of the separated SPBs in the period between SPB separation at the start of prophase until the metaphase anaphase transition. Analogue removal induced Plo1 activity on the G2/early mitotic SPBs (single dots) when the Cdc2.RL chimera had been recruited to the SPB via Cut12.NEGFP, but had no impact when no recruitment occurred. (e) Analogue wash out experiments of the indicated strains scoring the frequency of NETO status as described for Figure 4 b,c. (f) Analogue wash out experiments of the indicated strains as described for Figure 4b,c with the exception that the *cdc2.RLY15* allele that was used in these experiments, while retaining the F84G analogue sensitizing mutation, contained the wild type Y15 in place of the F15 mutation of *cdc2.RL* (Supplementary Figure 1c). This *cdc2.RLY15* allele therefore retained the ability to be subject to inhibitory phosphorylation by Wee1 kinase. Notably, there was no alteration of NETO status in the culture following the removal of analogue from cells in which this chimeric molecule had been recruited to SPBs via Cut12.NEGFP, establishing that MPF activity on the SPB is normally restrained by Wee1/Mik1 activity to prevent premature triggering of NETO. 40μM 3MB-PP1 was used for the Analogue wash out experiments presented here.

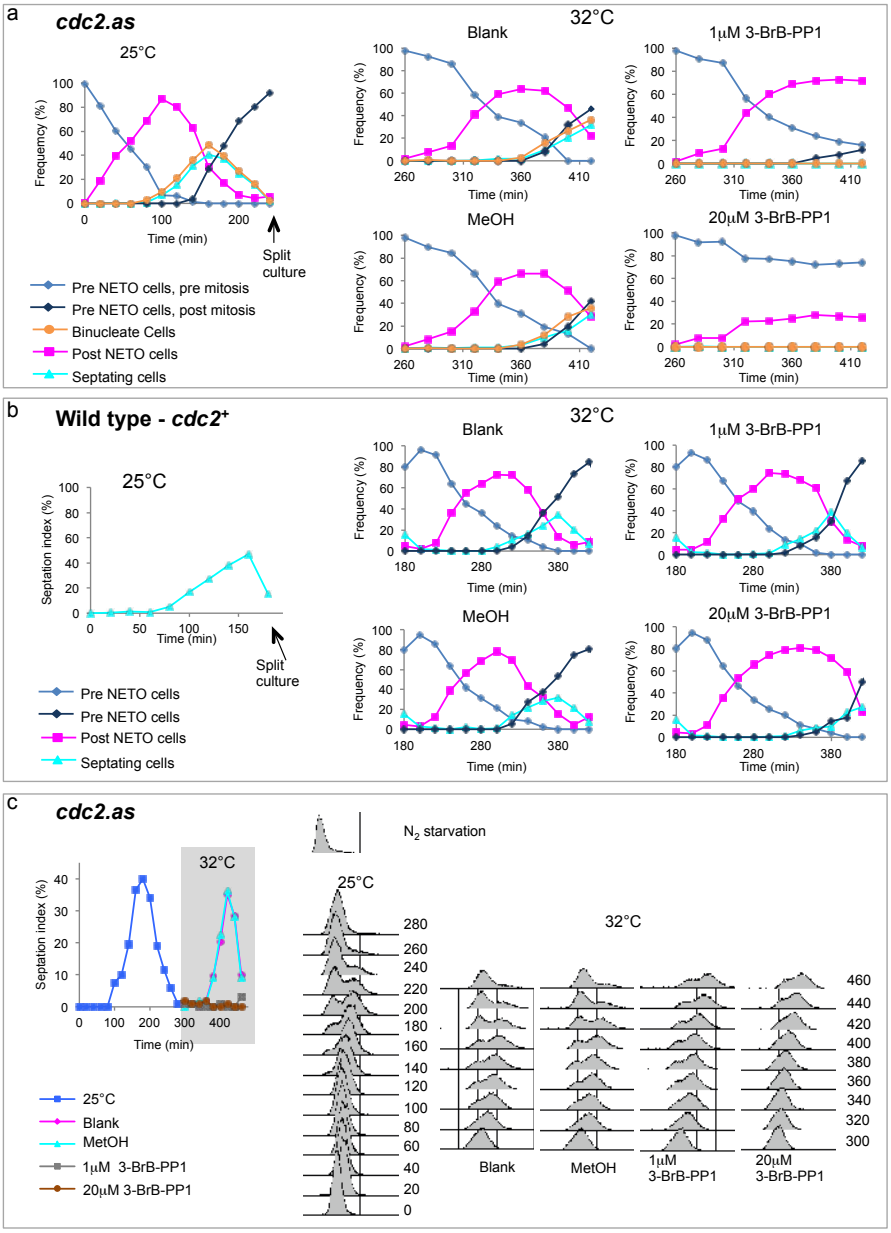

Figure S4 The MPF activity threshold for NETO induction lower than for mitotic induction. The control experiments for Figure 4a. (a) The same size selected culture as shown in Figure 4a. The 25°C panel shows the phenotypes from initial size selection until the splitting of the culture into four equal aliquots at 240 minutes, All cultures were shifted to 32°C to exploit the moderate temperature sensitivity of the *cdc2.as* mutation[11] and the addition of the ATP analogue 3-BrB-PP1 was used to compromise Cdc2 activity, as indicated, in the right hand panels. (b) Wild type control treatment that mirrored the *cdc2.as* regime for panel revealed that the addition of the ATP analogue 3-BrB-PP1 had no impact upon the timing of NETO even though 20 μM does lead delay the timing of mitotic commitment to a small degree. (c) A repeat of the experiment presented in Figure 4a in which size selected early G2 cells were allowed to transit one cell cycle before the early G2 cells were split into three aliquots and treated with the ATP analogue 3-BrB-PP1, the solvent methanol, or subjected to no treatment as indicated. The FACS profiles of DNA content show that the two analogue treated cultures remain in a G2 arrested state for the duration of the experiment. This shows that the inhibition of NETO does not arise from a secondary consequence of premature commitment to DNA replication which then blocks NETO via a checkpoint mechanism.

Supplementary Movies:

Movie 1: Plo1.GFP recruitment in *cut12*$^{+}$ and *cut12.s11*
Time lapse sequences of Plo1.GFP signals in *cut12*$^{+}$ (left) and *cut12.s11* (right) cells.

Movie 2: Photobleaching of Plo1.GFP signal at G2 SPBs; *cut12*$^{+}$ and *cut12.s11*
Time lapse sequences of Plo1.GFP signals on *cut12*$^{+}$ (left) and *cut12.s11* (right) SPBs following laser mediated photobleaching.

Movie 3: Plo1.GFP leaves the SPB of *cdc2.as* cells in a mixed *cdc2.as cdc2*$^{+}$ culture
The panel on the left identifies the *cdc2*$^{+}$ (red lectin) cells visualised in the first frame of the movie of this mixed culture. "+ATP analogue" indicates the timing at which 25mM 1NA-PP1 was added. Analogue remained present for the rest of the sequence. Analogue addition promoted the departure of the Plo1. GFP signal from the SPBs of *cdc2.as* but not the neighbouring *cdc2*$^{+}$ cells.
Movie 4: Plo1.GFP leaves the SPB of *cdc2.as* cells in a mixed *cdc2.as-cdc2*$^{+}$ culture at 32°C
The panel on the left/right identifies the *cdc2*$^{+}$ (red lectin) cells visualised in the first frame of the movie of this mixed culture. "+ DRUG" indicates the timing of analogue addition (25mM 1NA-PP1). Analogue remained present for the rest of the sequence. Analogue addition promoted the departure of the Plo1.GFP signal from the SPBs of the longer *cdc2.as* but not the neighbouring *cdc2*$^{+}$ cells. The moderate temperature sensitivity of the *cdc2.as* cells delayed mitotic commitment at 32°C.

Movie 5: Photobleaching reveals a stable association of Cut12.NEGFP anchored Plo1.RLTom and Cdc2.RLTom
Two cells are shown for each strain. Each cell shows a single focus of SPB associated fluorescence. The SPB of one of the cells was bleached. Each sequence runs for 20 minutes. There was no recovery. A single focal plane was captured every 4 seconds for 20 minutes for each sequence. Bleaching employed a 532nm 25mW laser to bleach the red fluorescence signal of the "Tomato" constructs and 488nm 25mW to bleach the green fluorescence of the "GFP" Cut12.NEGFP signal.